Conf-941101--12

UCRL-JC-118104
PREPRINT

Gas-Filled Targets for Large Scalelength Plasma Interaction Experiments on Nova

L. V. Powers
R. L. Berger
D. H. Munro
B. F. Lasinski
R. L. Kauffman
B. J. MacGowan
P. Amendt

C. A. Back
T. P. Bernat
S. N. Dixit
D. I. Eimerl
K. G. Estabrook
J. A. Harte
D. H. Kalantar

D. E. Klem
D. S. Montgomery
T. D. Shepard
R. E. Turner
L. J. Suter
R. E. Turner
E. A. Williams

J. C. Fernandez
W. W. Hsing
B. Wilde
Los Alamos National Laboratory
University of California
Los Alamos, NM 87545

B. H. Failor
Physics International
2700 Merced Street
San Leandro, CA 94577

This paper was prepared for submittal to the Proceedings of the 36th Annual Meeting of the American Physical Society, Division of Plasma Physics held November 7–11, 1994 in Minneapolis, MN.

November 1994

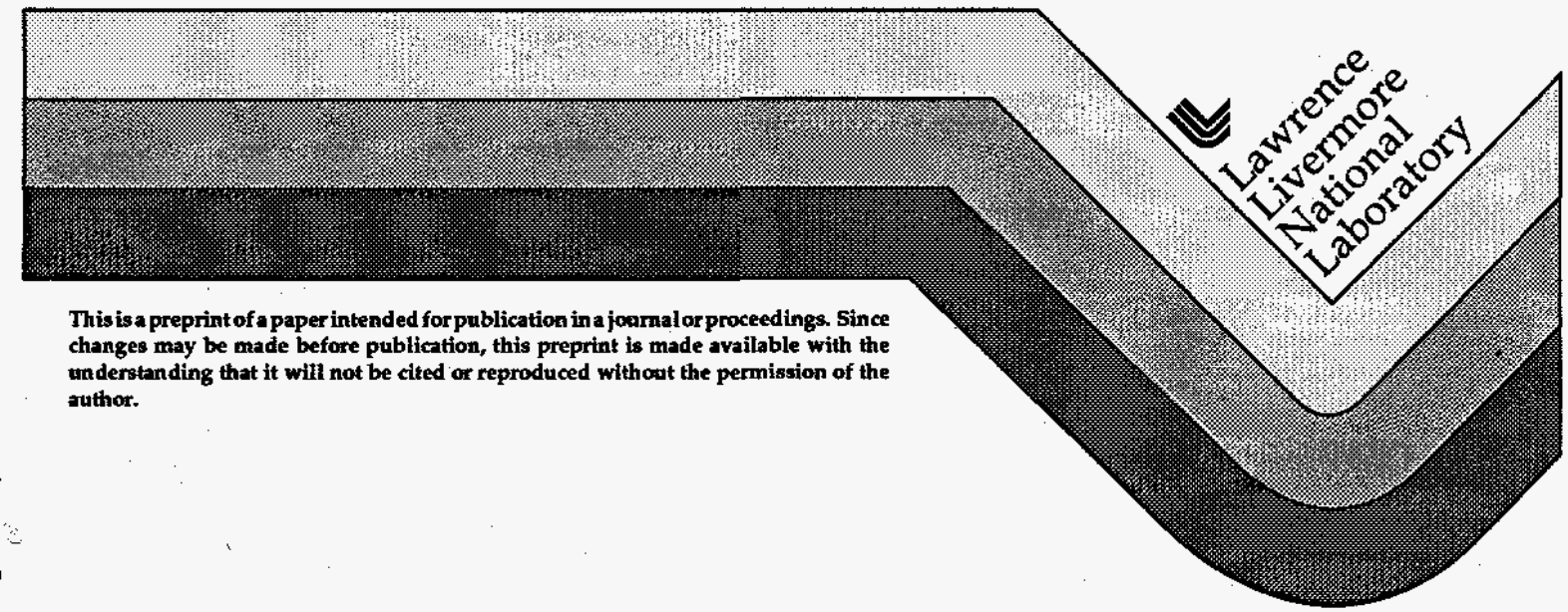

DISCLAIMER

Portions of this document may be illegible in electronic image products. Images are produced from the best available original document.

Gas-Filled Targets for Large Scalelength Plasma Interaction Experiments on Nova

L.V. Powers, R.L. Berger, D.H. Munro, B.F. Lasinski, R.L. Kauffman, B.J. MacGowan, P. Amendt, C.A. Back, T.P. Bernat, S.N. Dixit, D.I. Eimerl, K.G. Estabrook, J.A. Harte, D.H. Kalantar, D.E. Klem, D.S. Montgomery, T.D. Shepard, R.E. Turner, L.J. Suter, R.E. Turner and E.A. Williams
Lawrence Livermore National Laboratory

J.C. Fernandez, W.W. Hsing, and B. Wilde
Los Alamos National Laboratory

B.H. Failor
Physics International

Abstract

Stimulated Brillouin backscatter from large scale length gas-filled targets has been measured on Nova. These targets were designed to approximate conditions in indirect drive ignition target designs in underdense plasma electron density (n_e~10^{21}/cm^3), temperature (T_e>3 keV), and gradient scale lengths (L_n~2 mm, L_v>6 mm) as well as calculated gain for stimulated Brillouin scattering (SBS). The targets used in these experiments were gas-filled balloons with polyimide walls (gasbags) and gas-filled hohlraums. Detailed characterization using x-ray imaging and x-ray and optical spectroscopy verifies that the calculated plasma conditions are achieved. Time-resolved SBS backscatter from these targets is <3% for conditions similar to ignition target designs.

PACS numbers: 52.40.Nk, 52.50.Jm

Introduction

The proposed next-generation Inertial Confinement Fusion facility (NIF) is expected to produce moderate energy gain from direct and/or indirect-drive. Typical indirect drive target designs for NIF consist of spherical fuel capsules enclosed in cylindrical gold hohlraums [1]. Laser beams, arranged in cylindrical rings, heat the gold wall to produce x-rays which in turn heat and implode the capsule to produce fusion conditions in the fuel. In Nova hohlraums, moderate levels of stimulated Brillouin scattering (SBS) have been observed from plasma created by heating and expansion of solid material at the hohlruam wall [2]. For larger ignition targets, longer scale lengths of underdense plasma will be present. Hence maintaining low density in the hohlraum interior in order to control instability levels imposes an important constraint on target designs for NIF [1].

An important consideration in high-gain hohraum designs is maintaining adequate symmetry to efficiently implode high-convergence capsules. In vacuum, the expansion of the hohlraum wall over the duration of the NIF laser pulse (~18 ns) would produce unacceptable levels of asymmetry in the radiation field. Adequate symmetry is maintained in NIF hohlraums by filling the hohlraum interior with with low-density, low-Z gases. The gas is heated by the laser to produce a plasma with electron density of nearly $10^{21} cm^{-3}$ and electron temperature in excess of 3 keV. Once heated, the gas provides sufficient pressure to tamp the radiating gold surface. The laser beams propagate efficiently through the weakly absorbing, hot gas and deposit most (~90%) of the laser energy in high-Z hohlraum wall. However, even at this low density ($<n_c/10$ for laser wavelength λ=.351mm), worst-case estimates of stimulated Brillouin backscatter based on linear gain theory predict high SBS reflectivity.

We have designed and implemented experiments on Nova to quantify stimulated Brillouin backscatter for plasma and laser parameters that mimic indirect-drive NIF conditions. In these experiments, gas-filled targets are heated with 9 beams of the Nova laser to produce large, hot, nearly static plasmas. The tenth Nova beam, configured to emulate a single NIF beam, samples the preformed plasma. These plasmas have been extensively characterized using x-ray imaging and spectroscopy to verify the plasma conditions. These measurements compare favorably with calculations of the plasma conditions. The energy and spectra of light backscattered into the lens by the interaction beam are measured. The peak instantaneous backscatter fraction is <3% for laser conditions relevant to NIF. The backscattered spectra are consistent with the calculated plasma conditions and temporal evolution of the target parameters that influence SBS.

NIF plasma conditions

Indirect drive target designs for NIF [1] consist of cylindrical gold hohlraums filled with low-density He and containing a fuel capsule. The hohlraum wall is illuminated by two pairs of symmetrically placed rings of laser beams. The target geometry is shown in Ref. 1. In order to assess the susceptibility of these designs to parametric instabilities, we evaluate the various plasma parameters along the path of the laser. Quantities of interest are shown at the peak of the laser pulse (t=14.5ns) in Figure 1.

For these plasma conditions, stimulated Brillouin backscatter is the parametric process with the largest linear gain. Gains for other process of potential concern are estimated to be small. Stimulated Raman scattering is strongly Landau damped in the >3 keV underdense plasma. Two plasmon decay is controlled by strong density gradients near quarter-critical density. Filamentation is near

threshold, but calculations indicate that it can be stabilized by temporal beam smoothing techniques [3]. The estimated gain for sidescatter is substantially lower than for backscatter because the growth length is limited to the transverse dimension of the beam. Hence the strongest parametric process in the NIF targets is stimulated Brillouin backscatter.

To obtain the small signal intensity gain coefficient $G(\omega_s)$ we integrate the local intensity spatial gain rate, $\kappa(\omega_s,z)$ over the path of the scattered light. Calculated plasma parameters are used to evaluate the gain rate

$$\kappa(\omega_s,z)=\frac{(k_o-k_s)^2 v_o^2}{4\omega_o v_g}\,\mathrm{Im}\left(\frac{(1+\chi_i)\,\chi_e}{1+\chi_i+\chi_e}\right) \qquad (1)$$

at each point along this path. Here z is the position along the ray path, $\omega_{o,s}$ and $k_{o,s}$ are the frequency and wavenumber of the pump and scattered light waves respectively, $v_o \equiv eE_o/m\omega_o$ is the pump strength parameter, $v_g \equiv c^2 k_s/\omega_s$ is the group velocity of the ion acoustic wave, and $\chi_{e,i}$ are the electron and ion susceptibilities respectively. The gain rate includes enhanced ion Landau damping due to multiple ion species [4]. The intensity variation along the ray path due to beam divergence and inverse Bremsstrahlung is also included. For the NIF target, the maximum gain occurs at the peak of the laser pulse (t=14.5ns). For the parameters shown in Figure 1, the calculated gain coefficient is larger for the inner beam (G_{SBS}~30) because the average density is higher and the path length longer than for the outer beam (G_{SBS}~20). Whereas the calculated linear gains for NIF targets are large and suggest a possibility of unacceptable levels (~30%) of SBS backscatter, these calculations provide only an upper bound on the expected scattering. Nonlinear damping or detuning of SBS-produced ion waves is likely to be effective at gains well below the

calculated levels [5]. The intensity structure of spatially smoothed laser beams may limit the growth length [6]. Finally, the introduction of temporal beam smoothing can reduce the expected gain [6].

Two important limits of $G(\omega_s)$ are obtained if the plasma is compeletly uniform or if the plasma is very nonuniform. In the first case, the ion acoustic wave damping determines a constant gain rate over the length of plasma L. In the second case, the gain rate decreases as the waves become dephased over a region of size $\sim(v_i/\omega_a)L_v$. Setting the effective plasma size to the minimum of these two limits on the interaction length gives the approximate gain formula

$$G_{SBS} = \pi \times 10^{-16}\left(I\lambda^2/T_e\right)\left(n_e/n_c\right)\min\left(\frac{\omega_a}{v_i}\frac{L}{\lambda}, \frac{L_v}{\lambda}\right) \qquad (2)$$

where I is the laser intensity in W/cm^2, λ is the laser wavelength in microns, n_e/n_c is the electron density normalized to critical density, T_e is the electron temperature in keV, ω_a and v_i are the ion-acoustic-wave frequency and amplitude damping rate respectively, and $L_v \equiv Cs/|\partial v/\partial x|$ is the flow velocity gradient scale length. For NIF plasma parameters, the light ions in the gas provide efficient ion Landau damping ($v_i/\omega_a > 0.1$) [4]. Gradients in the flow velocity are weak in the direction of the beam propagation and do not further reduce the gain. By contrast, SBS is typically limited by velocity gradients in plasmas formed by exploding foils or solid targets, where the velocity gradient scale length is comparable to the plasma size. In addition, scalelengths ~1mm and electron temperatures ~0.5-2 keV which are typical in large scale length expanding plasmas [7], differ greatly from expected NIF plasma conditions, where the laser path is >2 mm and electron temperatures are >3 keV.

Consequently we have worked to produce plasmas that better approximate NIF conditions in which to test SBS scaling.

Nova target designs

Based on analysis of the NIF target design shown in the previous section, our goal was to produce target plasmas for SBS experiments with electron density $n_e \sim 10^{21}/cm^3$, electron temperature $T_e > 3$ keV, interaction length L~2 mm, and flow velocity gradient scale length $L_v > 6$ mm. In order to provide a stringent test of SBS, our objective was to produce a highly uniform, well characterized plasma that maintained the desired temperature and scale length for a duration of at least 0.5 ns. Various target options were investigated in simulations and evaluated according to these criteria. These included exploding foil geometries, plasmas formed between parallel exploding foils or expanding disks, low-density foams, and plasmas formed from low-Z (CH) liners in hohlraums, in addition to the gas targets that were fielded. The gas targets were selected for several reasons. Perhaps the most important consideration is that the NIF underdense plasma is formed by heating a low-density gas; hence we expect gas targets to most closely parallel the NIF plasma formation processes. Second, a substantial amount of Nova's energy would be required to expand a solid target to achieve the large scale length plasma required. Third, the initially homogeneous gas fill suggests less uncertainty and temporal variation in the plasma density than plasmas formed by expansion. Finally, the initially homogeneous gas targets are least susceptible to formation of small-scale, undetectable nonuniformities that could reduce SBS. Other target options, such as low-density foams and CH-lined hohlraums, appeared to be viable alternatives but have not been studied as extensively as the gas-filled targets.

The principal target types used were 1) gas balloons ~2.5-3 mm in diameter consisting of neopentane (C_5H_{12}) gas at 1 atm pressure, (10^{21} electrons/cm^3 when fully ionized) contained by a ~5000Å thick polyimide ($C_{22}H_{10}N_2O_5$) membrane, and 2) gold cylindrical hohlraums with length and diameter ~2.5mm with polyimide windows ~6000Å thick to contain the (neopentane) gas. Gas target geometries similar to these were proposed by Denavit and Phillion [8]. Diagrams of these two targets are shown in Figure 2. An alternative hohlraum geometry was used in complementary experiments fielded on Nova by LANL [9]. Using nine beams of Nova which deliver ~30kJ of 0.351μm light, we heat the gas to preform plasmas with the desired parameters. The tenth beam is an interaction beam whose intensity, pulse shape, f-number, and "smoothness" are varied. The SBS backscatter intensity and spectrum (and the SRS spectrum) from the interaction are measured with time resolution of 100ps and spectral resolution of 1Å.

In order to reach the desired temperature, coupling of the laser energy to the gas must be efficient and losses to kinetic energy (e.g., plasma expansion and window heating) must be modest. Heating the 10mm^3 volume of target to the desired temperature requires coupling 12 kJ of Nova's ~30 kJ of energy to the gas. Heating these gas targets with 0.351μm light at average intensity of ~10^{15} Watts/cm2 proves nearly optimal. The heater beams are arranged to maximize energy coupling to the gas by maximizing the pathlength of the laser in the gas. For a 3 mm-diameter gasbag, for example, the inverse Bremsstrahlung absorption length is equal to the initial target diameter when T_e reaches ~2 keV (at t~500psec in design calculations) and is uniformly heated to ~3 keV by t~800ps. The gasbag target disassembles as a rarefaction wave moves in from the plasma edges. The time required for the rarefaction to reach the target

center is ~$L/2C_s$=5ns at T_e=3 keV, so that a significant plateau (~2mm) of plasma at the desired density remains by the time the gasbag temperature becomes uniform. Using green illumination (λ_l=0.503μm) for plasma formation was considered for easier discrimination of optical scattering from the 3ω interaction beam. Plasma formation with 2ω heater beams proved undesirable, however, in part because the more efficient absorption of 2ω light results in longer laser burnthrough times and faster target disassembly, leading to a shorter effective scale length for interaction experiments and a less homogeneous plasma. Another consideration is that the initial electron density of the gas, when fully ionized, is near quarter-critical density for 2ω light, prompting concern that parametric instabilities could alter the energetics of the plasma formation process.

Although the gasbag and hohlraum targets are similar in gas volume and composition, and achieve similar underdense plasma conditions, each target also has unique features. In the gasbag targets, access for plasma heating and diagnostics is nearly ideal. Because the heater beams can be arranged to symetrically illuminate the entire target surface, a very uniform plasma temperature and density that is ideal for physics scaling experiments is produced. Imaging diagnostics provide multiple views of the target expansion. The rarefaction from the large surface area of the target, however, requires that the volume be heated quickly with a flattop laser pulse and limits the lifetime of uniformly heated, millimeter scale length plasma to <1 ns.

In hohlraum targets, laser access is limited to laser entrance holes (LEHs) in the ends of the cylinder. Consequently the contained gas is heated partially by thermal conduction. The gradients in density and temperature which are

introduced by the asymmetric heating are calculated to be weak in the direction of laser propagation. One motivation for fielding two targets with similar underdense plasma conditions for SBS studies is to test whether inhomogeneities introduced by nonuniform heating in hohlraums or interaction of the laser with high-Z blowoff from the hohlraum wall affects SBS behavior in an unexpected way. Containment of the gas by the walls, on the other hand, increases the plasma lifetime and allows heating with a shaped pulse that reduces the likelihood of exciting parametric processes in the (initially) cold gas. The high-Z hohlraum walls also procude x-ray signals that provide reliable diagnostics of beam propagation through the gas and hot electron generation.

The detailed plasma conditions for both the Nova targets are obtained from 2-dimensional LASNEX [10] simulations. Standard LASNEX models are used for Lagrangian hydrodynamics, laser absorption, deterministic radiation transport, flux limited (f=.05) diffusion electron transport, and NLTE atomic physics. Standard simulations are cylindrically symmetric about the beam axis, although alternative (2-dimensional) geometries have been used to model azimuthal variations that are important to understand some diagnostic data. The generic behavior of the two targets is similar, although details differ due to the different geometries and pulse shapes. The laser burns through the polyimide membrane in ~200 psec; the gas becomes transparent by t~500 psec. The path length of the $n_c/10$ density plateau decreases from ~2mm at t=500 psec to ~1.5 mm at t=1ns. The electron density ($10^{21}/cm^3$) and temperature (~3 keV) along the beam path calculated by LASNEX, are uniform over a pathlength L~2 mm. The maximum calculated flow velocity in this region is $<10^7$cm/sec. Later in time the pathlength of the $n_c/10$ density plateau decreases due to rarefaction. The heater pulse duration (1ns for gasbags / 1.4 ns for hohlraums) is too short to allow for

complete electron-ion equilibration; the ratio T_i/T_e rises from ~0.1 at t=0.8ns to ~0.2 at the end of the pulse (compared to ~0.4 at the peak for the NIF pulse). This temporal variation is significant because the ion wave damping in neopentane varies significantly over this range of T_i/T_e [4]. Detailed profiles from the simulations are compared with the NIF target design in Figure 3. Table 1 summaries this comparison for quantities that determine the linear SBS gain coefficient.

Table 1: Comparison of selected plasma parameters for Nova gas-filled targets and NIF target designs

	Gasbag	Hohlraum	NIF
interaction length $\int^{n<n_c} dl$	~2 mm	~2 mm	~ 3 mm
line density $\int^{n<n_c} (n_e/n_c)\, dl$	~ 0.3 mm	~ 0.2 mm	~ 0.3 mm
electron temperature	3 keV	3 keV	5 keV
ion/electron temperature ratio	0.1	0.1	0.4
gain coefficient G_{SBS}	30	22	21

The values shown are shown at the time corresponding to the maximum of the calculated SBS gain. The Nova plasma parameters are within ~50% of the NIF values except for the ion/electron temperature ratio, which is lower in the Nova targets due to the shorter time available for electron-ion equilibration to occur. This difference leads to larger calculated ion acoustic wave damping ν_i in NIF [4] The increased damping and slightly higher electron temperature of the NIF compensate for the longer beam pathlength to give similar SBS gain coefficients to the Nova experiments for the same laser intensity ($2X10^{15}$ Watts/cm^2). Interaction beam intensities ranged from $1X10^{15}$ to greater than $5X10^{15}$ Watts/cm^2 in Nova experiments. For the highest intensities, the calculated gain exceeds that of NIF targets by more than a factor of 2.

Characterization using x-ray diagnostics

Extensive characterization was carried out to ensure that predicted plasma conditions were achieved. Spectroscopic measurements are consistent with the calculated underdense plasma temperatures. Imaging techniques confirm the plasma size, homogeneity, and temporal evolution. Streaked and gated images show that the heater beams propagate through the gas as calculated without significant breakup. Finally, optical spectra are consistent with expected target parameters and evolution.

Doped fibers or foils were mounted in the targets as a diagnostic of electron temperature. The dopants were chosen to maximize sensitivity over the calculated temperature range. The electron temperature was inferred from both single-element and isoelectronic line ratios[9]. From recorded spectra of emission from the dopants, the electron temperature was inferred from both single-element and isoelectronic line ratios [11]. Dopants were chosen for sensitivity to the calculated temperature variation. Detailed analysis of the isoelectronic ratios from Ti/Cr and K/Cl spectra confirms that $T_e > 3$ keV in the directly illuminated gas during the interaction pulse [12]. Gated spectra were also obtained from foils in a position in the hohlraum target that was not directly illuminated by the laser. These measurements indicate delayed heating outside of the beam path, but verify that electron conduction provides good temperature uniformity by t~1ns in agreement with LASNEX simulations.

For gasbag targets, streaked and gated x-ray images provided a record of the target evolution [13]. The target diameter as a function of time is inferred from the size of the emitting region in streaked 1-dimensional images of >3 keV x-ray emission. The good agreement between this observation and simulations also

supports the inference that the gas has reached the calculated ~3 keV temperature. In addition, images were used to monitor the large-scale uniformity of the preformed plasmas. In both observations and simulations, the standard illumination geometry using large, overlapping heater beams produced uniform images consistent with a large, homogeneous central region of plasma, while targets illuminated with smaller, discrete laser spots showed considerable structure.

In the gasbag targets, the onset of x-ray emission at different target positions is a qualitative measurement of the heater beam propagation, but the overlapping geometry of the heater beams precludes accurate determination of the laser propagation rate. In the hohlraum targets, x-ray emission from several target views provide evidence that the heater beams propagate as calculated. X-ray diagnostics are filtered to collect 2-3 keV emission to sample line emission for Ar and Cl dopants in the gas, as well as M-band emission from the gold hohlraum wall. Early in time, gated images of Ar/Cl line emission through the laser entrance hole show heated channels in the gas corresponding to the paths of the propagating beams. The size of these channels and the image contrast agree well with predictions from LASNEX calculations. Gated images through a slot in the hohlraum wall provide a direct view of the footprint of two overlapping laser beams. The onset of emission and the axial extent of the beam footprint agree well with the calculated wall emission. Streaked spectra were recorded through the laser entrance hole at 62° relative to the hohlraum axis. Line emission from Ar/Cl dopants in the neopentane gas is observed early in the laser pulse after the membrane over the laser entrance hole has been ablated. Later at t~1ns, gold M-band emission is seen from the heated wall viewed by the diagnostic. In all cases the temporal history and spatial extent of the x-ray emission are consistent

with LASNEX modeling of beam propagation and wall heating. The measured and calculated M-band emission history are compared in Figure 4.

Characterization from optical spectra

Optical spectra for both SBS and SRS back through the lens of the interaction beam were recorded with a grating spectrometer streak camera combination . These signals provide information about the parameters and evolution of the plasma. Model spectra are generated using plasma parameters calculated by LASNEX as input to calculate spectrally- and temporally-resolved gain and reflectivity. We have compared measured spectra with model spectra for a variety of configurations of the interaction beam. An example is shown in Figure 5 for a gasbag target. For this case, the interaction beam intensity was $2X10^{15}$ W/cm^2. The interaction beam pulse shape was trapezoidal with ~300 psec rise and fall and ~600 psec flattop, with a ~600 psec delay relative to start of the heating beams, and was typical for these experiments. Typical SRS spectra have a distinct feature corresponding to the $n_c/10$ density plateau (λ_{SRS}=5700Å), and in some cases a weaker feature corresponding to a density of ~$0.15n_c$. In calculations this feature is associated with the compression shock generated by the expanding polyimide membrane. The measured SBS spectra vary both in intensity and wavelength over the duration of the interaction pulse. When the interaction beam turns on, a strong unshifted feature which we interpret as scattering from remnants of the membrane is observed. This interpretation is supported by a hohlraum experiment in which one heater beam was redirected to preheat the portion of the membrane encountered by the interaction beam and the unshifted feature was greatly reduced. Later, as the density of the membrane material decreases, the dominant scattering comes from the $n_c/10$ density plateau and the spectrum is red-shifted. The observed shifts are consistent with

the predicted $\Delta\lambda$~8Å for a 3 keV, static plasma when SBS is strong and are somewhat smaller under conditions where scattering is weak. By contrast, SBS spectra from exploding foils or disks are typically blue-shifted indicating that the signal is dominated by plasma regions where $V_{\|} > C_S$. In both gas targets, the peak scattering occurs at ~1 ns and decreases while the interaction beam is still at its peak intensity. Modeling suggests that in gasbags this reduction is primarily due to a decrease in the size of the scattering region in time. A similar reduction in the hohlraums, where rarefaction effects are less important, is caused by increasing ion Landau damping late in the pulse.

SBS reflectivity

The fraction of backscattered light near the laser frequency was measured with time-integrating calorimeters. For these experiments, the interaction beam was configured to closely mimic a four-beamlet NIF beam cluster in focal length (f/8), intensity ($2X10^{15}$ Watts/cm^2), beam smoothing (RPP's [14] and four-color temporal smoothing [15]). The peak SBS reflectivity into the lens was ~3% for both the gasbag targets and the hohlraum targets. In addition, scalings in f-number (f/4 and f/8), intensity (1-5 X 10^{15} Watts/cm^2), and temporal beam smoothing (1-color, 4-color with 4.4Å line separation, and SSD with 3.5Å bandwidth) were investigated. The backscattered light fractions from these experiments [16, 17] are shown in Figure 6.

SBS measurements from the f/4 interaction beam showed the expected scalings: the reflectivity increased with intensity and decreased when temporal beam smoothing was introduced. The reflectivities were lower from hohlraum targets than from gasbag targets for the same nominal intensity. This is consistent with linear gain calculations and arises from differences in the focussing geometries:

for the hohlraums, best focus was in low-density, flowing plasma at the LEH, whereas in the gasbags best focus was in the $n_c/10$, stationary plasma at the target center. For these large plasmas, beam divergence produces a significant drop in intensity across the scattering region. Peak SBS reflectivities with f/8 interaction beams were ~3% for neopentane-filled targets. There is no clear reduction of the SBS by the four-color bandwidth, but in gasbag targets SSD was effective in reducing the reflectivity at intensities ~$2X10^{15}$ Watts/cm^2. Higher backscatter was observed from a target filled with deuterated neopentane (C_5D_{12}) and CO_2, consistent with the expected reduction in ion Landau damping in gases without hydrogen [4].

The scattering levels with f/4 and f/8 interaction beams are well below the levels expected based on linear theory in the neopentane-filled targets. For gain coefficients of >20, the calculated reflectivity would reach the pump depletion limit of ~30% reflectivity in the absence of other nonlinear saturation mechanisms. For these large gains, however, nonlinear saturation mechanisms which limit the amplitude or coherence of the ion waves driven by SBS [5] are likely to be important. Scattering outside the 3° collection cone of the f/8 lens may be significant. Filamentation, which is near or above threshold in the f/8 experiments [6], could spread backscattered light into a larger cone. This spreading effect also account for the apparent insensitivity of the reflectivity to the four-color bandwidth. Theoretical and experimental work are underway to quantify this effect.

Summary

Using gas-filled targets, we have preformed plasmas with Nova which closely match the calculated plasma environment in NIF hohlraums in electron density

and temperature, density and velocity scale lengths, and calculated SBS gain. These plasmas were extensively characterized using x-ray and optical diagnostics. The observed target evolution agrees well with predictions from LASNEX simulations. These comparisons both verify that the desired parameters for SBS experiments were attained, and corroborate important aspects of our modeling of NIF hohlraum conditions. SBS reflectivity from an interaction beam is <3% when the interaction beam mimics the NIF laser beam intensity, focussing, and beam smoothing.

Acknowledgments

The authors acknowledge valuable discussions with J. Kilkenny, J. Lindl, and M. Rosen. We acknowledge the LASNEX group for facilitating the simulations required to design and analyze these experiments. The contributions of Nova laser scientists in developing and implementing beam modifications, and Nova operations personnel in conducting the experiments, were indispensable. The gas-filled targets are the culmination of a significant target development effort by Luxel Corporation and the LLNL target fabrication group. G. Stone was instrumental in coordinating target fabrication and delivery. This work was performed under the auspices of the U.S. DOE by Lawrence Livermore National Laboratory under Contract No. W-7405-Eng-48.

References :

[1] Steven W. Haan, Stephen M. Pollaine, John D. Lindl, Laurance J. Suter, Linda V. Powers, Richard L. Berger, Edward Alley, George Zimmerman, Peter A. Amendt, W. Kirk Levedahl, Richard A. Sacks, Aleksei I. Shestakov, George L. Strobel, Steven Weber, William Krauser, Nelson M. Hoffman, Douglas Wilson and David Harris, "Design and modeling of ignition targets for the National Ignition Facility", in this issue of Physics of Plasmas.

[2] J.C. Fernandez, J.A. Cobble, W.W. Hsing, B.H.Wilde, B.H. Failor, R.G. Hockaday, P.L. Gobby, D.A. Montgomery, H.N.Kornblum and J.L. Miller, Los Alamos National Laboratory Report # LACP94-144.

[3] R.L. Berger, B.F. Lasinski, T.B. Kaiser, E.A. Williams, A.B. Langdon, and B.I. Cohen, Phys. Fluids B **5**, 2243 (1993).

[4] E.A. Williams, R.L. Berger, A. V. Rubenchik, R.P. Drake, B.S. Bauer, D.D. Meyerhofer, and T.W. Johnston (submitted to Physics of Plasmas).

[5] W. L. Kruer, Phys. Fluids **23**, 1273 (1980)

[6] R.L. Berger, Bull. Am. Phys. Soc. **38**, 2012 (1993).

[7] H.A. Baldis, D.S. Montgomery, J.D. Moody, C. Labaune, S.H. Batha, K.G. Estabrook, R.L. Berger and W.L. Kruer, Plasma Phys. Controlled Fusion **34**, 2077 (1992) and references therein.

[8] J. Denavit and D.W. Phillion, Phys. Plasmas **1**, 1971 (1994).

[9] J.C. Fernandez, private communication.

[10] G. Zimmerman and W. Kruer, Comments Plasma Phys. Controlled Fusion **2**, 85 (1975).

[11] R.S. Majoribanks, M.C. Richardson, P.A. Jaanimagi, R. Epstein, Phys. Rev. A **46**, 1747 (1992).

[12] C.A. Back, E.J. Hsieh, R.L. Kauffman, D.H. Kalantar, D.E. Klem, R.W. Lee, B.J. MacGowan, D.S. Montgomery, L.V. Powers, T.D. Shepard, L.J. Suter, G.F. Stone and R.E. Turner (submitted to Phys. Rev. E).

[13] D.H. Kalantar, D.E. Klem, B.H. Failor, W.W. Hsing, B.J. MacGowan, J.D. Moody, D.S. Montgomery, D.H. Munro, T.D. Shepard and G.F. Stone, submitted to RSI.

[14] S.N. Dixit, I.M. Thomas, B.W. Woods, A.J. Morgan, M.A. Henesian, P.J. Wegner and H.T. Powell, Applied Optics **32**, 2543 (1993).

[15] D.M. Pennington, M.A. Henesian, R.B. Wilcox, T.L. Weiland, R.B. Ehrlich, C.W. Laumann, D. Eimerl and H.T. Powell, Technical Digest CLEO'94 **8**, 161(1994).

[16] B.J. MacGowan, C.A. Back, R.L. Berger, K.S. Bradley, J.D. Colvin, S.N. Dixit, D.I. Eimerl, K.G. Estabrook, B.H.Failor, M.A. Henesian, W.W. Hsing, D.H. Kalantar, R.L. Kauffman, D.E. Klem, W.L. Kruer, J.L. Miller, D.S. Montgomery, J.D. Moody, D.H. Munro, T.J. Murphy, D.M.Pennington, L.V. Powers, T.D. Shepard, G.F. Stone, R.J. Wallace, T.W. Weiland, R.B. Wilcox, S.C. Wilks and E.A. Williams, Proceedings of the IAEA 15th International Conference on Plasma Physics and Controlled Nuclear Fusion Research, IAEA-CN-60, 1994.

[17] L.V. Powers, R.E. Turner, R.L. Kauffman, R.L. Berger, P. Amendt, C.A. Back, T.P.Bernat, S.N. Dixit, D.I. Eimerl, J.A. Harte, M.A. Henesian, D.H. Kalantar, B.F. Lasinski, B.J. MacGowan, D.S. Montgomery, D.H. Munro, D.M. Pennington, T.D. Shepard, G.F. Stone, L.J. Suter and E.A. Williams, submitted to Phys. Rev. Lett.

Figure captions

1) Lineouts of plasma parameters in NIF hohlraum along beam paths of inner (solid line) and outer (dashed line) beam paths.

2) Schematic diagram of Nova target geometries for a) gasbag targets and b) hohlraum targets. The gray shading shows the beam geometry.

3) Comparison of calculated plasma parameters along the beam paths for the inner cone of NIF beams (gray line), Nova hohlraums (solid line), and gasbags (dashed line).

4) a) Emission spectra of ~3 keV x-rays viewed through the laser entrance hole at 68° from the hohlraum axis.
b) Temporal lineouts of gold M-band emission (hv=3.2 keV) from data (light line) and calculation (solid line).

5) Comparison of a) observed and b) calculated emission spectra for SBS.

6) SBS reflectivities from a) gasbag targets and b) hohraum targets with f/8, RPP interaction beam.

Figure 1

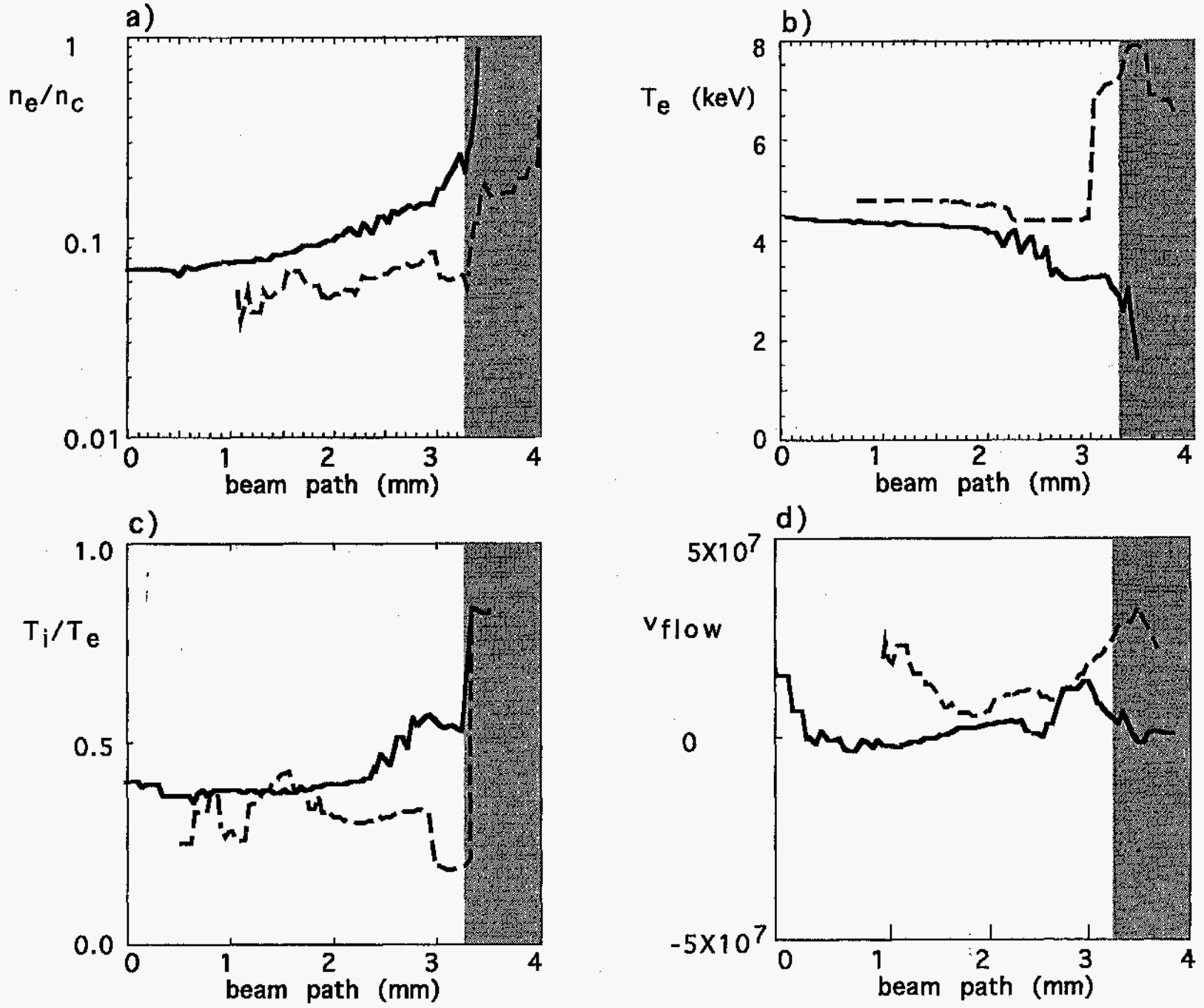
a)
1
n_e/n_c
0.1
0.01
0
1
2
3
4
beam path (mm)
b)
8
T_e (keV)
6
4
2
0
0
1
2
3
4
beam path (mm)
c)
1.0
T_i/T_e
0.5
0.0
0
1
2
3
4
beam path (mm)
d)
$5X10^7$
v_{flow}
0
$-5X10^7$
0
1
2
3
4
beam path (mm)

Figure 2

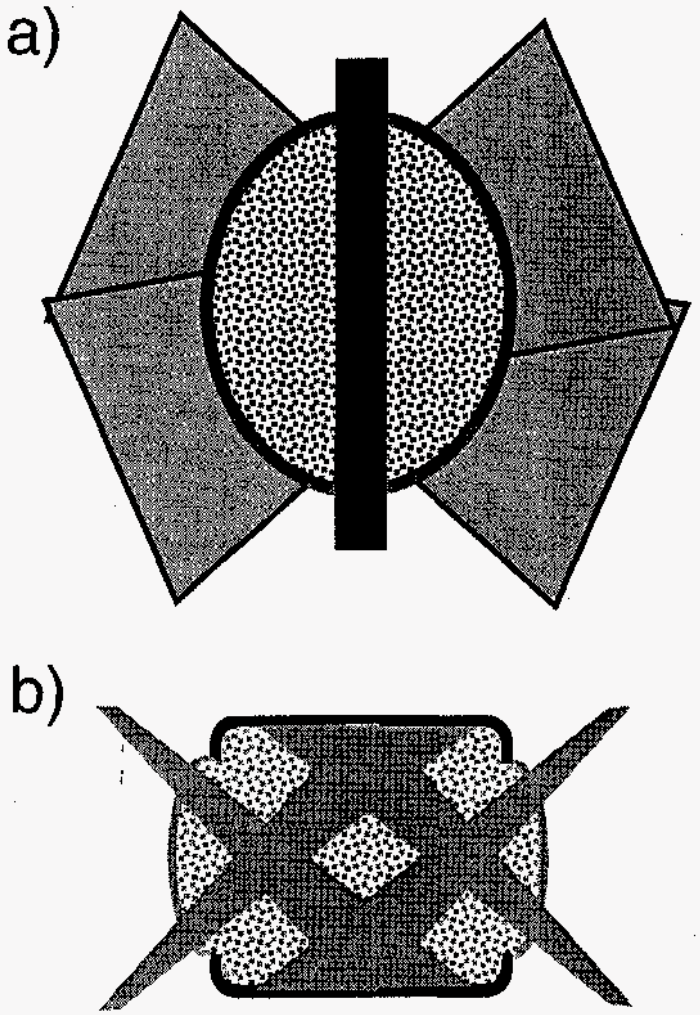

Figure 3

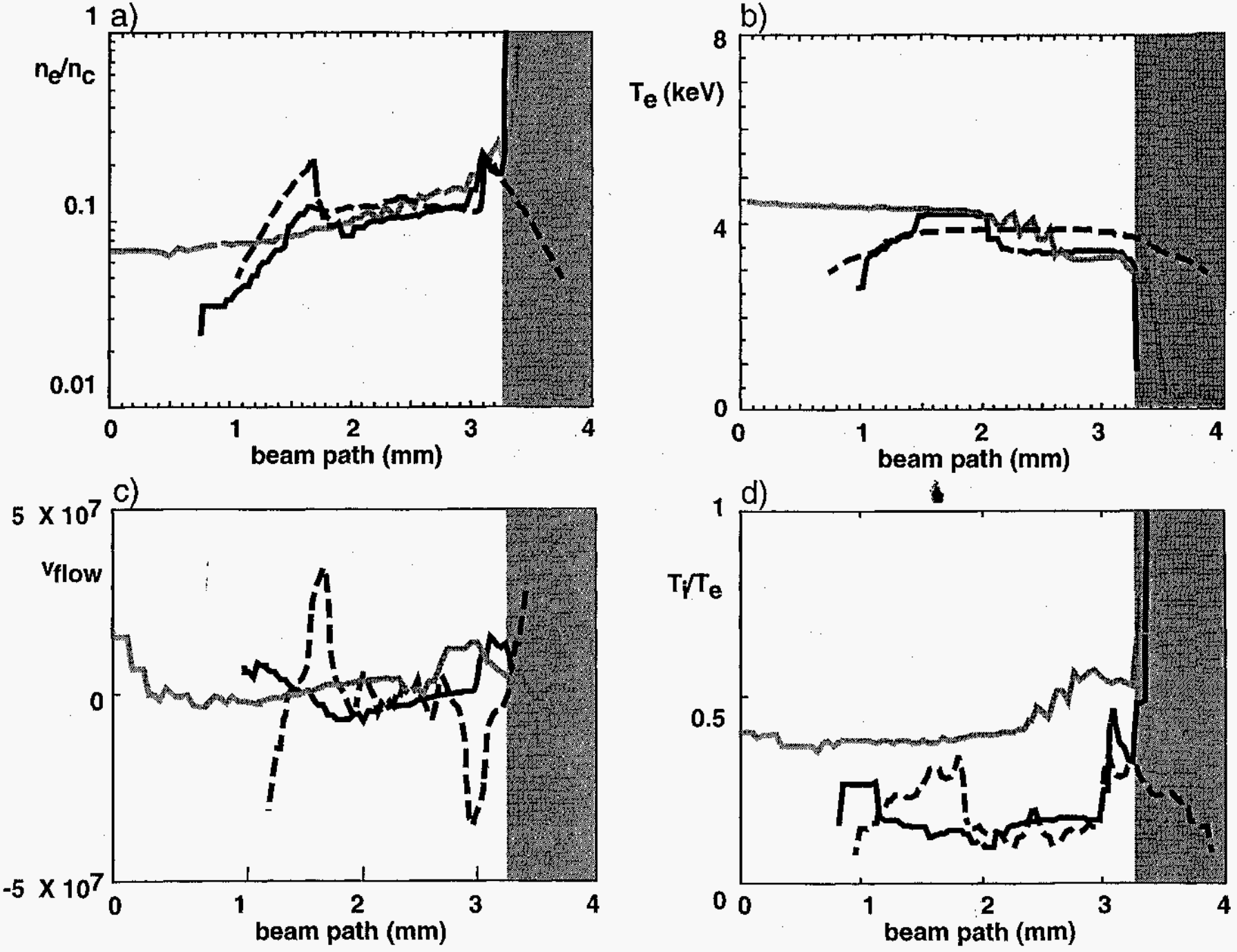
a)
1
n_e/n_c
0.1
0.01
0
1
2
3
4
beam path (mm)
b)
8
T_e (keV)
4
0
0
1
2
3
4
beam path (mm)
c)
5 X 10^7
v_{flow}
0
-5 X 10^7
0
1
2
3
4
beam path (mm)
d)
1
T_i/T_e
0.5
0
0
1
2
3
4
beam path (mm)

Figure 4

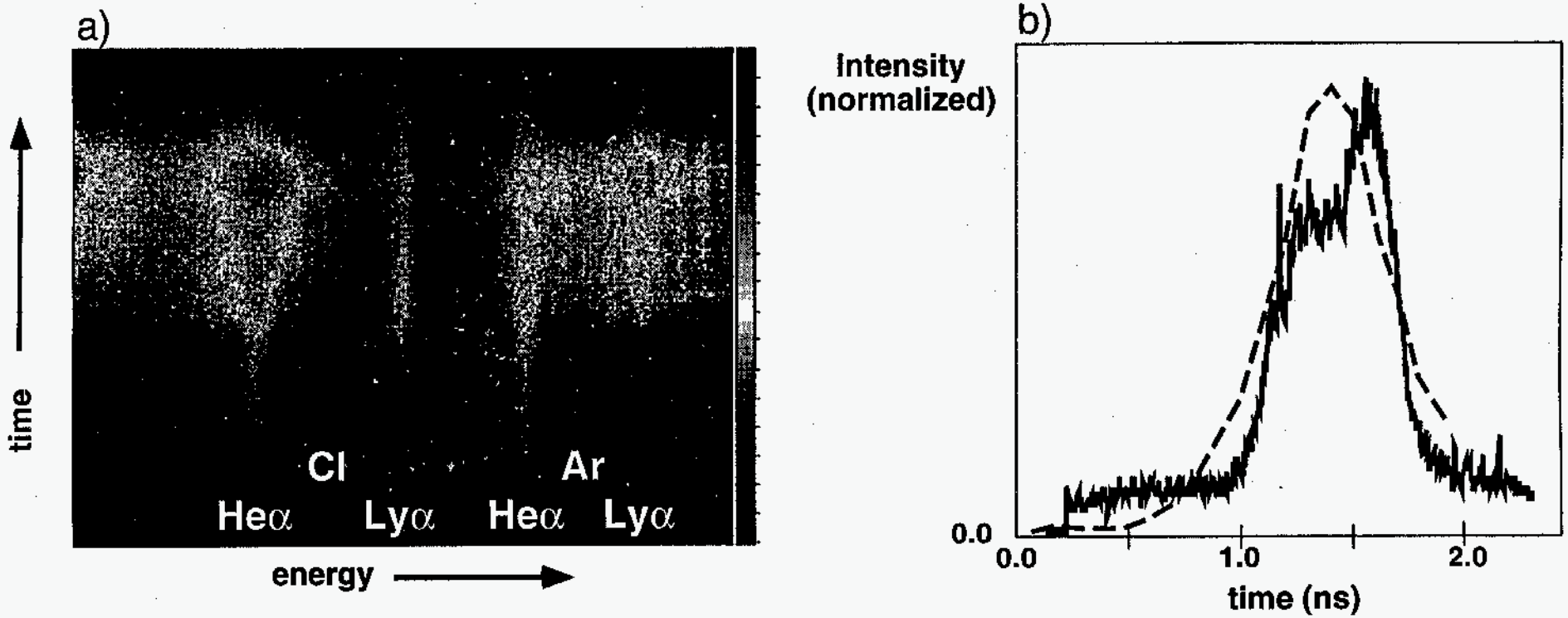
a)
time
Cl
Ar
Heα
Lyα
Heα
Lyα
energy
b)
Intensity
(normalized)
0.0
0.0
1.0
2.0
time (ns)

Figure 5

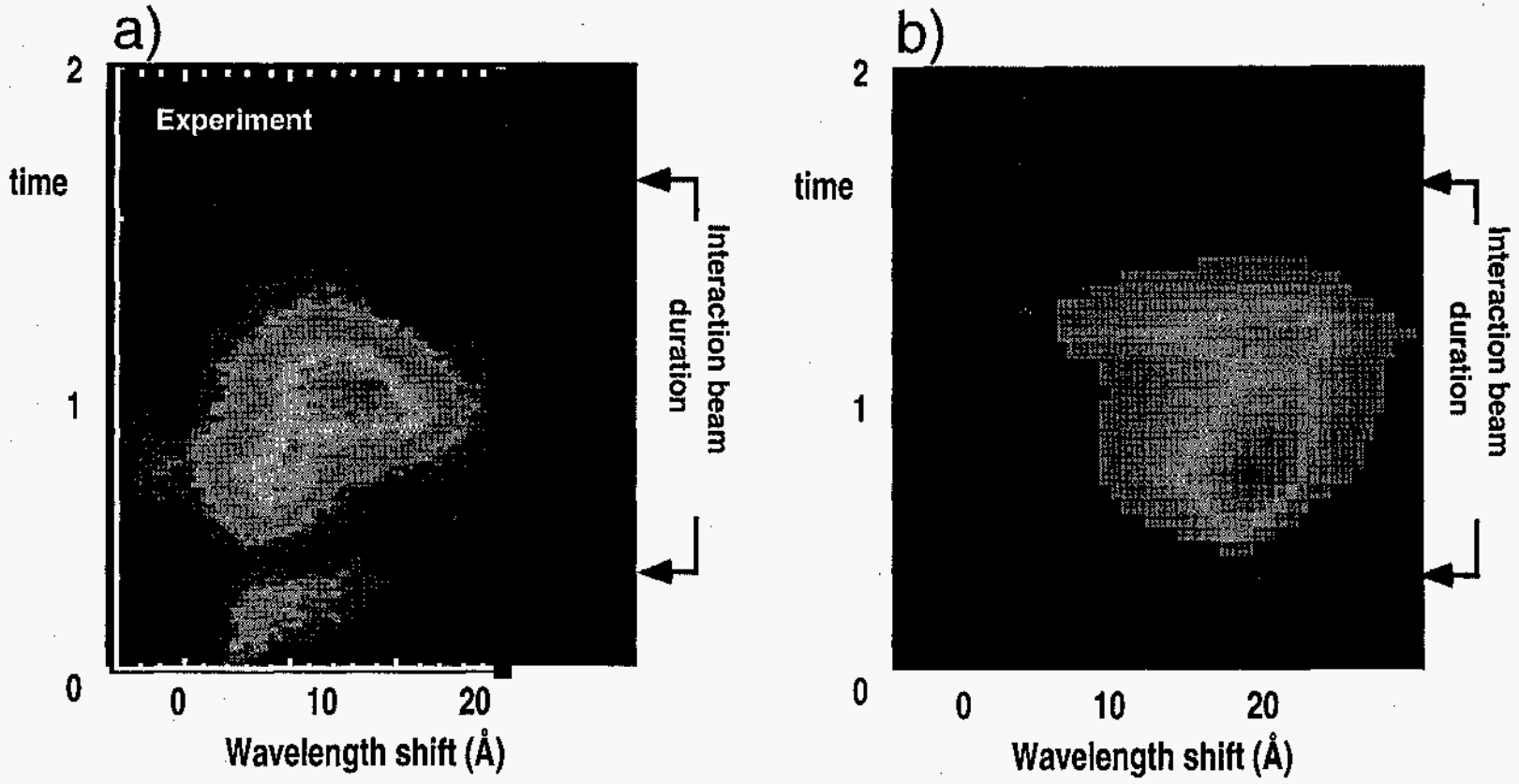
a)
Experiment
time
2
1
0
0
10
20
Wavelength shift (Å)
Interaction beam duration
b)
time
2
1
0
0
10
20
Wavelength shift (Å)
Interaction beam duration

Figure 6

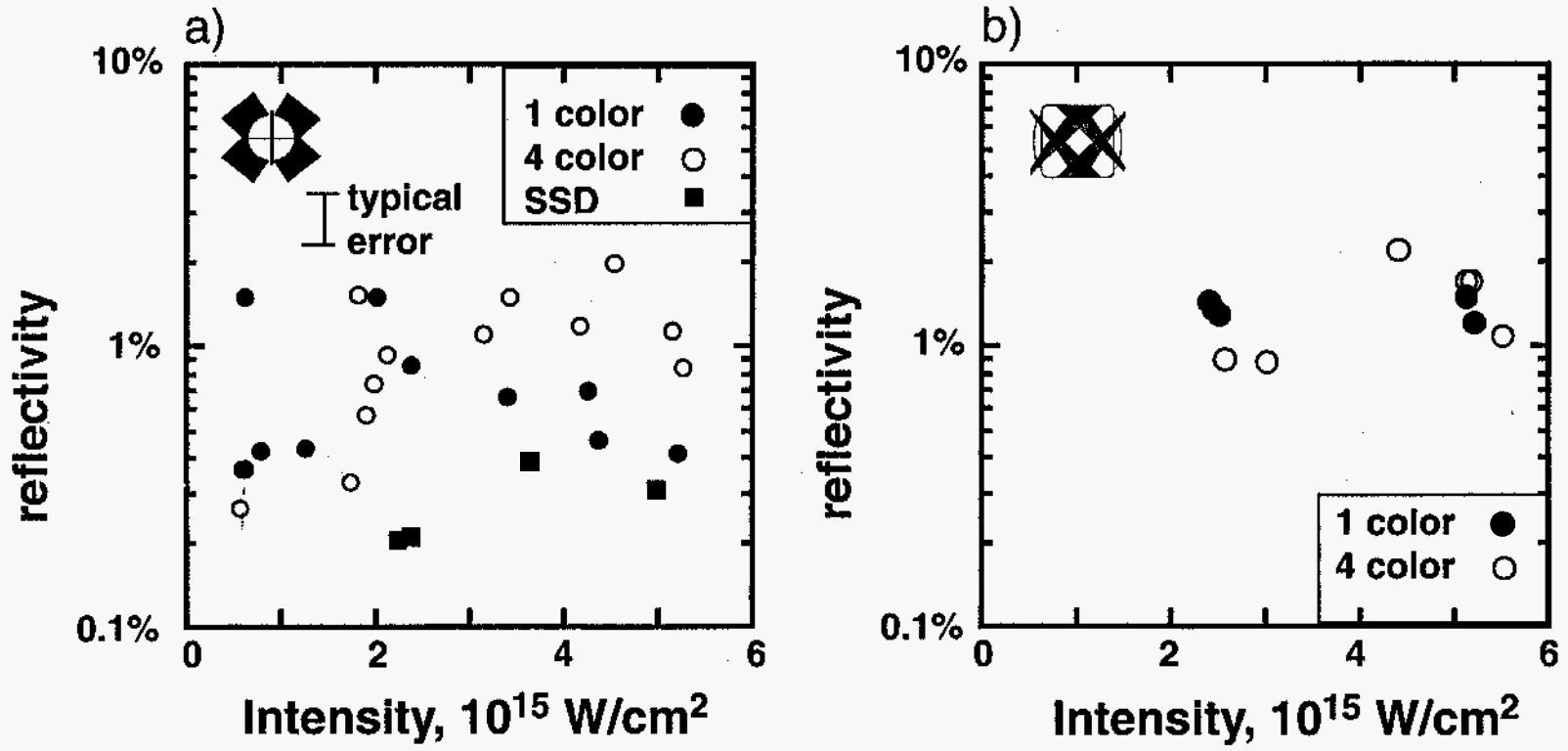

RELK 0594-21A